Journal of Photochemistry and Photobiology A: Chemistry 222 (2011) 314–322

Contents lists available at ScienceDirect

Journal of Photochemistry and Photobiology A: Chemistry

journal homepage: www.elsevier.com/locate/jphotochem

Photocatalytic behavior of WO_3-loaded TiO_2 systems in the oxidation of salicylic acid

Mehdi Ismail[a,b], Latifa Bousselmi[a], Orfan Zahraa[b,*]

[a] Centre de Recherches et des Technologies des Eaux, Technopôle de Borj Cedria B.P. 273, 8020 Soliman, Tunisia
[b] Laboratoire Réactions et Génie des Procédés, CNRS-Nancy Université, ENSIC, 1 rue Grandville, B.P. 20451, F-54001 Nancy Cedex, France

ARTICLE INFO

Article history:
Received 29 March 2011
Received in revised form 10 June 2011
Accepted 1 July 2011
Available online 14 July 2011

Keywords:
TiO_2
WO_3
Salicylic acid
Photocatalytic activity
Sol–gel

ABSTRACT

The role of WO_3 in enhancing the photocatalytic activity of TiO_2 deposits has been investigated through the oxidation of salicylic acid using UV and vis-light irradiation. Different procedures of semiconductor loading and deposition were undertaken: firstly, TiO_2-Degussa P25 was impregnated with tungstic acid solution and spread on the glass substrate. Secondly, precursor of WO_3 was ammonium paratungstate, mixed with a monomer and spincoated on the glass. Finally, a gel of WO_3–TiO_2 was synthesized by sol–gel method and spincoated on the glass, $TiCl_4$ was used as the titanium dioxide precursor and ammonium paratungstate was introduced in the sol before precipitation of TiO_2.

The films obtained were characterized by UV–vis spectrophotometry, X-ray powder diffraction and scanning electron microscopy in order to better understanding the behavior and the effective role of WO_3.

A red-shift in the absorption edge wavelength was observed for coupled catalysts prepared by the first procedure, the bang gap energy decreased to respectively 2.7 and 2.6 eV for 0.5% and 2.5 wt.% of WO_3. A tendency to agglomeration and a higher percentage of rutile in the catalysts were observed after WO_3 loading. The photocatalytic activity under visible light increased consequently for catalysts with 2.5 wt.% of WO_3 and variable inhibition was observed for lower loadings, but only a positive effect of WO_3 was observed under UV light. The inhibition of photocatalysis was also observed under visible light for some WO_3 loadings for coupled catalysts prepared by the procedure 2 and a great enhancement was observed at the 0.5 wt % of WO_3 under UV light.

Concerning the catalysts prepared by the sol–gel method, a positive effect of the WO_3 introduction was noted: the coverage on the glass was improved, the band gap energy decreased to 2.3 eV with 4 wt.% of WO_3 and the corresponding photocatalytic activity was remarkably enhanced under visible light. A higher photocatalytic activity and a better response to WO_3 introduction was also observed under UV irradiation. The introduction of tungsten precursor before the crystallization of TiO_2 seems to be an appropriate method to ensure good contact and better charge transfer between the two semiconductors. As expected, the photocatalytic performances were generally higher under UV light than under visible light for all the catalysts and 0.5 wt.% WO_3–TiO_2 was the common optimal loading for the 3 procedures exhibiting the best activity under UV light.

1. Introduction

The degradation of organic pollutants in water by photocatalysis, using semiconductor powders as photocatalysts has been extensively studied during recent years. It has been shown that titanium dioxide (TiO_2) was an excellent photocatalyst because of its high activity, chemical stability and low cost [1–5]. However, the photocatalytic activity of TiO_2 (with band gap of 3.2 eV and excited by photons with wavelengths under 387 nm) is still limited to irradiation by UV wavelengths [6], so that photocatalytic process does not occur effectively during the irradiation with solar light as only about 4% of the total radiation of the solar spectrum is in ultraviolet region [7,11]. Therefore modification of TiO_2 in the view to obtain a higher light absorption by shifting absorbance to the visible wavelengths has become the aim of many authors [7–10]. One of the methods is the coupling of TiO_2 with other semiconductors such as TiO_2/CdS [15,16], TiO_2/SnO_2 [8,17], TiO_2/ZnO [18] and TiO_2/WO_3 [7–9,12–14,19–21,24].

Another challenge concerns the authors: catalyst powders used in suspended state in water, especially the nanometer-scale TiO_2

---

* Corresponding author. Tel.: +33 3 83 17 51 18; fax: +33 3 83 32 29 75.
E-mail address: Orfan.Zahraa@ensic.inpl-nancy.fr (O. Zahraa).

1010-6030/$ – see front matter © 2011 Elsevier B.V. All rights reserved.
doi:10.1016/j.jphotochem.2011.07.001

(Degussa P25), require a supplementary separation step which limits their practical reuse. Immobilization of catalysts on a substrate may be an appropriate solution to avoid such post treatments.

In recent years, numerous works have been done on the coupling of TiO_2 by WO_3 and preparation methods were very different, such as wet impregnation [8,12–14,19,21], sol–gel [9,20], ball milling [7] and grafting of tungsten alkoxides [24]. Many deposition techniques were also used to obtain the catalyst deposits such as simple deposition, spin coating, electrospinnig and dip coating. All these preparation procedures influence the dispersibility of WO_3 particles in the titanium dioxide powder, their coverage on the surface of TiO_2, their size and their exposure to the light source and may induce consequently differences in authors' results, which are also function of the light source (UV, Vis). Actually, under a visible light, a better performance using WO_3–TiO_2 system was found by the majority of reviewed papers [7–9,13,14,19,21]. However, under UV light, the effect of WO_3 addition lead to contradictory results: a better efficiency of WO_3–TiO_2 was found for the photocatalytic degradation of monocrotophos [7], acid Red [19], stearic acid [20] and toluene [21], but inhibition was observed for the degradation of 4-chlorophenol [8], phenol [15], 2-naphthol and gaseous CH_3CHO [28] and formic acid [29].

Our contribution in this work is to give more insights on the behavior of TiO_2–WO_3 is a function of preparation procedures, precursors and light sources. Accordingly, three different procedures were followed to prepare coupled catalysts that offer a higher photocatalytic performance than unloaded TiO_2 toward the oxidation of salicylic acid (SA) in aqueous solution. Home manufactured and commercial TiO_2, loaded by WO_3 produced from two different precursors as well as two deposition techniques (simple deposition and spin coating) were combined, which allows us in an original work to find the most suitable preparation procedure and to try to link photocatalytic performances to the characteristics of the catalysts. The SA was selected to act as a model compound since it is widely used in pharmaceutical and cosmetic preparations (e.g., skin-care products and cosmetic emulsions) and in food industries (generally as a preservative), and this product may be found in wastewaters and have possible effects on health and environment [25].

2. Materials and methods

2.1. Materials

TiO_2 (P25, Degussa), titanium tetrachloride [$TiCl_4$] (98%, Fluka), tungstic acid [H_2WO_4] (99%, Aldrich) and ammonium paratungstate [$(NH_4)_{10}H_2W_{12}O_{42}4H_2O$, commercially called APT] (>99%, Riedel de Haën) were used as purchased without further purification. The pollutant model was the salicylic acid (SA) [$C_7H_6O_3$] (≥98%, Fluka).

2.2. Analysis

The absorption of catalysts over the entire spectrum (200–700 nm) was monitored in a UV-Vis spectrophotometer (Shimadzu UV-3600) equipped with an integrating sphere (diameter: 150 mm, type: LISR-2100). The structure of catalysts was characterized by X-ray diffraction technique (XRD) using the "Panalytical" instrument (X'Pert Pro MPD). The SEM diagrams were obtained from Jeol T330 equipped with a XRD Synergy system. Salicylic acid concentration was monitored by HPLC on a chromatograph equipped with a Shimadzu SPD-6A spectrophotometric detector adjusted to the wavelength of 295 nm, corresponding to the maximal absorption of SA. A Lichrosob column was used and elution was carried out by a mixture of methanol (70%) and water (30%) [27].

2.3. Film preparation procedures

All the coupled titania samples were deposited on a substrate which consisted in a flat plate of ordinary glass 4 cm × 48 cm purchased from "Leroymerlin". The substrate was pre-treated with dilute nitric acid and washed with NaOH solution in order to increase the density of OH groups on the surface of the glass which enhances the binding of TiO_2, then rinsed by distilled water and finally dried. Coupling TiO_2 by WO_3 and deposition were carried out according three different procedures:

Procedure 1: this is the incipient wetness method of Lin and Kwon et al. [8,13], it consists briefly on the following steps: TiO_2-powder (P25 Degussa, $4\,g\,L^{-1}$) was suspended under vigorous stirring in a dilute ammonia solution, which was allowed to dissolved with a stoichiometric amount of tungstic acid (H_2WO_4), the suspension was then deposited on the glass substrate, dried in the air and fired at 450 °C during 4 h. The same deposition procedure was repeated three times so as to obtain a thick layer with deposed specific mass of about $0.2\,mg\,cm^{-2}$ ($\pm 0.05\,mg\,cm^{-2}$), above this value it was demonstrated that the rate of photocatalytic degradation of SA with TiO_2-P25 deposit was constant [22].

Procedures 2 and 3: these two procedures consisted in spin coating deposition of the catalysts on the same glass substrate by a spin coater machine, a speed set to 1500 rotations per minute. A viscous form was needed in order to use this deposition method; for this reason a powder of TiO_2-P25 with paratungstate $(NH_4)_{10}H_2W_{12}O_{42}4H_2O$ was mixed with a monomer ($C_{12}H_{10}O_4$ called HDDA) in the second procedure, and a viscous gel of WO_3/TiO_2 was prepared via sol–gel method in the third procedure according the following step: a 0.05 mol $TiCl_4$ was dissolved in 100 ml absolute ethanol under vigorous stirring, then diluted by 150 ml of water. The ammonium paratungstate powder was introduced at this step according to the choosing molar ratio. Afterwards, the ammonia solution was dropped into the $TiCl_4$/ethanol/water/APT solution and the titanic acid gel precipitated. The gel was rinsed and separated by centrifugation until the Cl^- ions could not be detected. Then a H_2O_2 solution (30 wt.%) was added drop-wise to the gel under vigorous stirring until a yellow and viscous solution was obtained, which was suitable for spin coating deposition.

Only one deposition was done with spin coating method and deposed specific mass was about $0.07\,mg\,cm^{-2}$ ($\pm 0.02\,mg\,cm^{-2}$) and $0.2\,mg\,cm^{-2}$ ($\pm 0.05\,mg\,cm^{-2}$) respectively for films prepared by the second and the third procedure. All catalyst deposits were dried and fired in air at 450 °C during 4 h, annealing temperatures in the same range (400–500 °C) were used for the preparation of coupled WO_3/TiO_2 catalysts [8,12–14,19,20].

2.4. Photocatalytic tests

The photocatalytic reactor (Fig. 1) consisted in a parallepiped vesselwith the catalyst fixed on a flat glass Plate 4 cm × 48 cm placed on the bottom, as detailed elsewhere [22]. Photocatalytic activities of prepared samples were tested for decomposition of 250 ml salicylic acid (SA) aqueous solution running freely on the plate with a debit of $220\,ml\,min^{-1}$. The initial concentration of SA was fixed to $10\,mg\,L^{-1}$ (arbitrary value) and monitored by HPLC chromatography. Two different light sources were used for photocatalytic tests: UV and white lamps. The UV lamp (Philips-TLD,

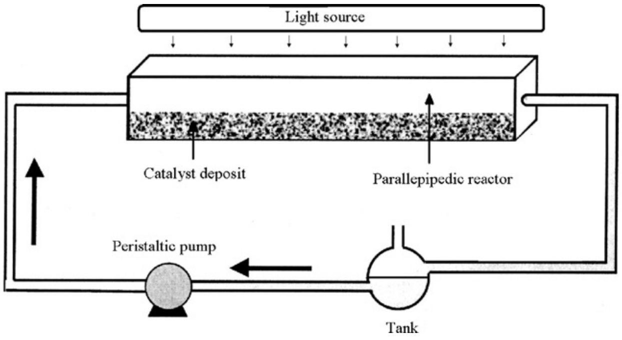

Fig. 1. Scheme of experimental setup for the photocatalytic degradation.

18 W, 56 cm long) emits in the range of 350-390 nm with a maximum at around 365 nm having an intensity of 2.83 W m^{-2}. The white lamp (Osram-L, 18 W, 56 cm long) provides mainly visible light in the range of 400–600 nm and insignificant amount of UV at 365 nm (0.13 W m^{-2}).

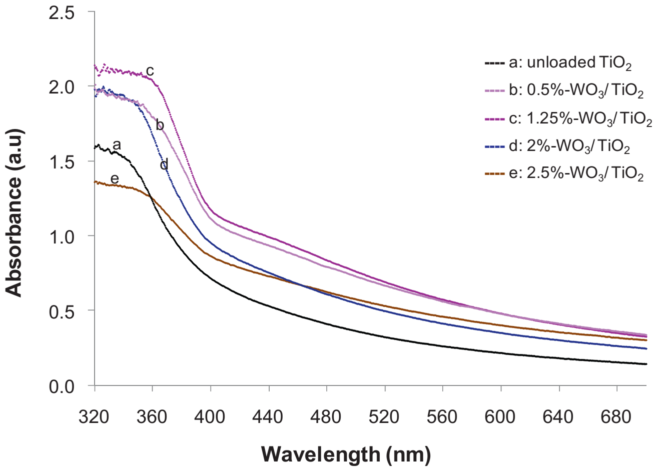

Fig. 2. The UV–vis spectrum of coupled WO_3/TiO_2 catalysts prepared by Procedure 1.

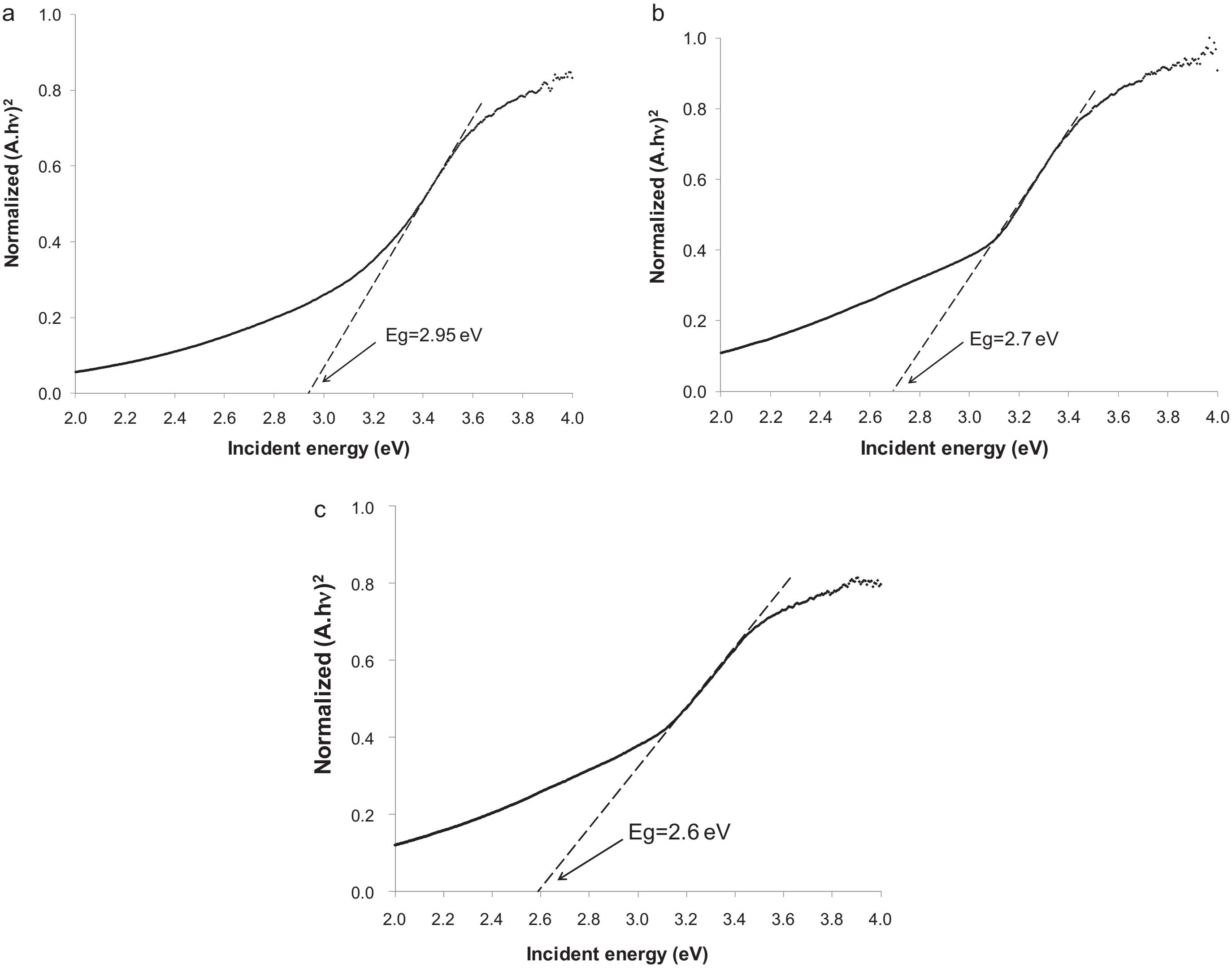

Fig. 3. (a) Normalized $(Ah\nu)^2$ versus incident energy for unloaded TiO_2. (b) Normalized $(Ah\nu)^2$ versus incident energy for 0.5%-WO_3/TiO_2. (c): Normalized $(Ah\nu)^2$ versus incident energy for 2.5%-WO_3/TiO_2.

3. Results and discussion

3.1. Characterization of the catalysts

Since the coupled catalysts prepared by Procedure 1 were manually deposed on the glass substrate in a suspension state, the visual appearance of the films was as not uniform with non homogeneous thickness: no difference was observed between loaded and unloaded TiO_2 which was still creamy white and opaque after calcination. The catalyst was hardly removed by the hand from the glass substrate which indicated a good adhesion.

Catalysts prepared by Procedure 2 and 3 presented a good visual uniformity with homogeneity in thickness, white color, and more transparence compared to ones of Procedure 1 but the adhesion on the glass substrate was not excellent.

The UV–vis spectra of coupled catalysts prepared by the Procedure 1 (Fig. 2) showed a high optical absorbance in the region of 400–700 nm owing to the thick layer of the deposits, absorption peaks were observed in the region of 320–400 nm corresponding to the usual region of TiO_2 absorption. The absorption edge wavelengths can hardly be determined as shown in Fig. 2 but their shift to the red direction is clearly observed after WO_3 loading.

Tauc's expression for a direct optical transition, $\alpha h\nu = C(h\nu - E_g)^{1/2}$ [30] was used to measure the optical energy band gap (E_g), where α is the absorption coefficient, C is a constant and $h\nu$ is the photon energy. Assuming a direct optical transition and considering the proportionality between the absorbance (A) and the absorption coefficient (α) [30], $(Ah\nu)^2$ was plotted as a function of the photon energy ($h\nu$) and the linear part of those graphs was extrapolated to the energy axis, allowing to determine E_g (Fig. 3) [20,23,30–32]. The values of E_g are obviously approximate since extrapolation of the linear part may not be accurate in some cases.

The estimated band gap energy of unloaded TiO_2 (2.95 eV) could not be right since it is slightly lower than the value cited in literature (between 3.12 eV and 3.2 eV) [8,9,23].

E_g evolution with WO_3 loading for catalysts prepared by the Procedure 1 is presented in Fig. 4a, a decrease of band gap energy was generally observed. By coupling the TiO_2 nanoparticles with WO_3, we were able to lower the band gap energy of unloaded TiO_2 from 2.95 eV to respectively 2.7 and 2.6 eV for 0.5% and 2.5 wt.% of WO_3. The value of band gap energy at 2.5 wt.% loading (2.6 eV) is equal to one reported by Lin [8] who has measured the band gap energy of 3 wt.%-WO_3/TiO_2 prepared in similar conditions (fired at 400 °C and same precursors).

The UV–vis spectra of coupled catalysts prepared by the Procedure 2 were similar to those of the unloaded TiO_2 (not shown) and the band gap energy did not change consequently (about 3.1 eV). However, the band gap energy decreased considerably until the value of 2.3 eV with 4 wt.% of WO_3 for catalysts prepared by the Procedure 3 (Fig. 4b). It should be noticed that the band gap energy of unloaded TiO_2 prepared by sol–gel method was found to be equal to 2.8 eV, less than the regular value: this result is expected since a higher density of defects is usually found in the sol–gel manufactured TiO_2 [33].

The SEM images of the coupled semiconductors prepared by Procedure 1 were compared to the ones of unloaded TiO_2. The catalysts having lower band gap energies were chosen to investigate the morphology. The 2.5 wt.%-WO_3 loaded TiO_2 exhibits a larger agglomeration size and more uniform morphology than unloaded TiO_2. The appearance of unloaded TiO_2 and 0.5 wt.%-WO_3 loaded TiO_2 is nearly similar (Fig. 5). Lin et al. and Kwon et al. [8,13] have also reported uniform morphology for coupled 3 wt.%-WO_3/TiO_2 system, their preparation method was similar to one used in this work (Procedure1). Lin also observed larger particles size of coupled catalysts (about 300 nm [8]) than of pure TiO_2 (20–30 nm [4,8,13]) but that observation was not found by Kwon who did not noticed any change in lattice fringes of WO_3/TiO_2 particles [13].

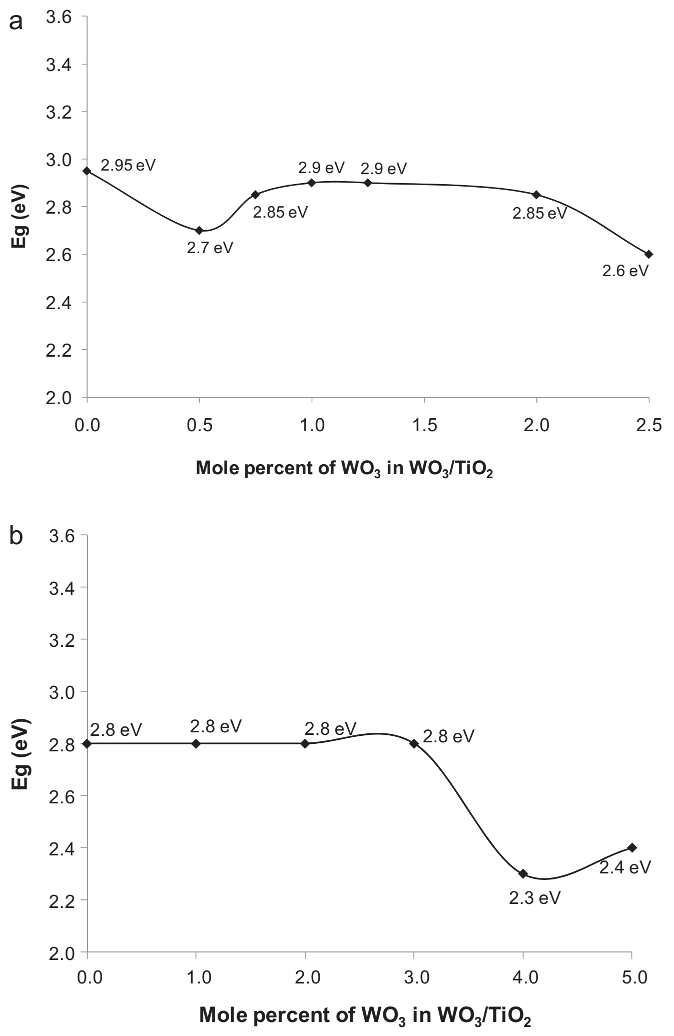

Fig. 4. (a) Evolution of estimated band gap energy with different WO_3 loadings (coupled catalysts prepared by procedure 1), (b) evolution of estimated band gap energy with different WO_3 loadings (coupled catalysts prepared by procedure 3).

Only the SEM analysis of the coupled semiconductors prepared by Procedure 3 was investigated and compared to ones of Procedure 1, since the method was completely different (sol–gel method) and TiO_2 was produced from $TiCl_4$ which is different from P25 samples used in Procedures 1 and 2.

In Fig. 6a, it can be observed that the TiO_2 particles prepared by sol–gel method exhibit non uniformity in shape and have no homogeneous coverage of the glass support. The coverage of the substrate was easily obtained in the Procedure 1, since manual deposition was employed. In addition, loading by WO_3 seems to improve the coverage (Fig. 6b and c) with a higher agglomeration size obtained for 4 wt.%-WO_3/TiO_2 loaded catalysts.

XRD analysis (not shown) of catalysts prepared by the Procedure 1 revealed that unloaded TiO_2 consisted of mostly the anatase phase (about 91%) and that the rest was rutile, but a higher amount of rutile (between 20% and 26%) was found for all coupled catalysts (see Table 1). XRD diagrams of TiO_2 and coupled WO_3/TiO_2 were exactly the same; the diffraction peaks of WO_3 could not be found, and this result may be explained by the high dispersion of the few WO_3 particles in the bulk phase of the catalyst [7] and/or their incorporation into the TiO_2 in the WO_3/TiO_2 system

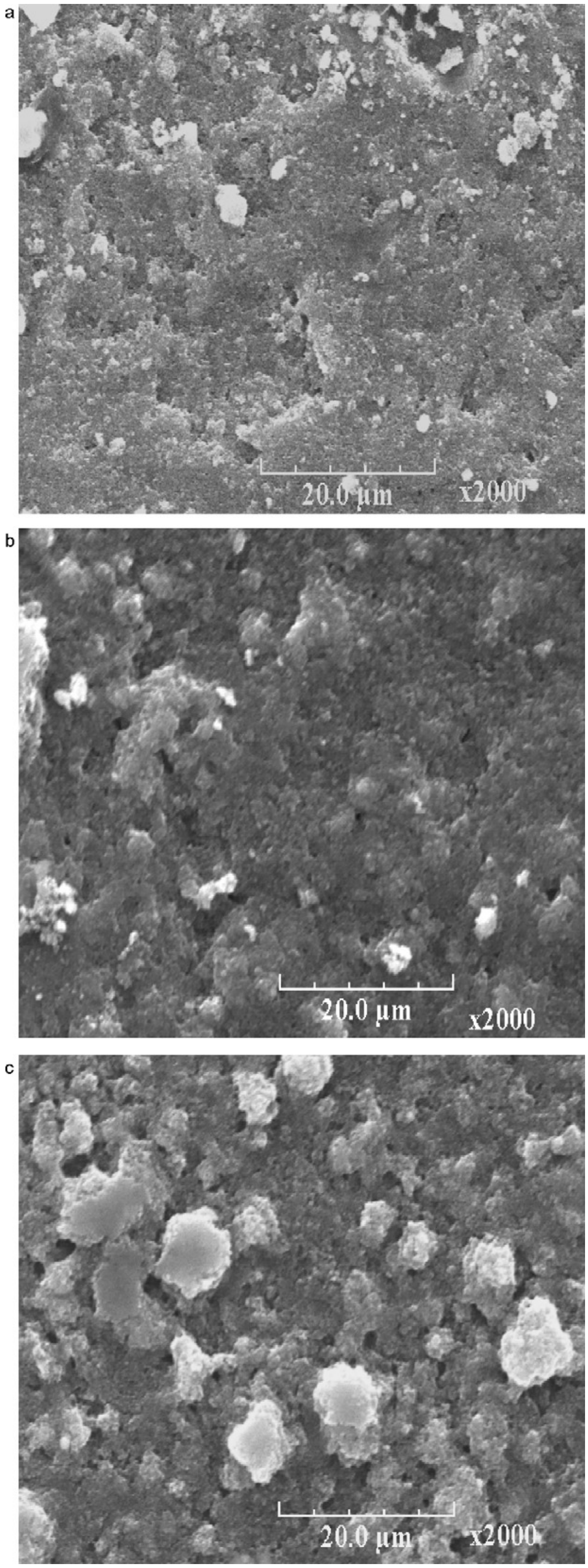

Fig. 5. (a) SEM diagrams for coupled WO_3/TiO_2 catalysts prepared by Procedure 1: unloaded TiO_2, (b) SEM diagrams for coupled WO_3/TiO_2 catalysts prepared by Procedure 1: 0.5% – WO_3 loaded TiO_2 and (c) 2.5% – WO_3 loaded TiO_2, and (c) SEM diagrams for coupled WO_3/TiO_2 catalysts prepared by Procedure 1: 2.5% – WO_3 loaded TiO_2.

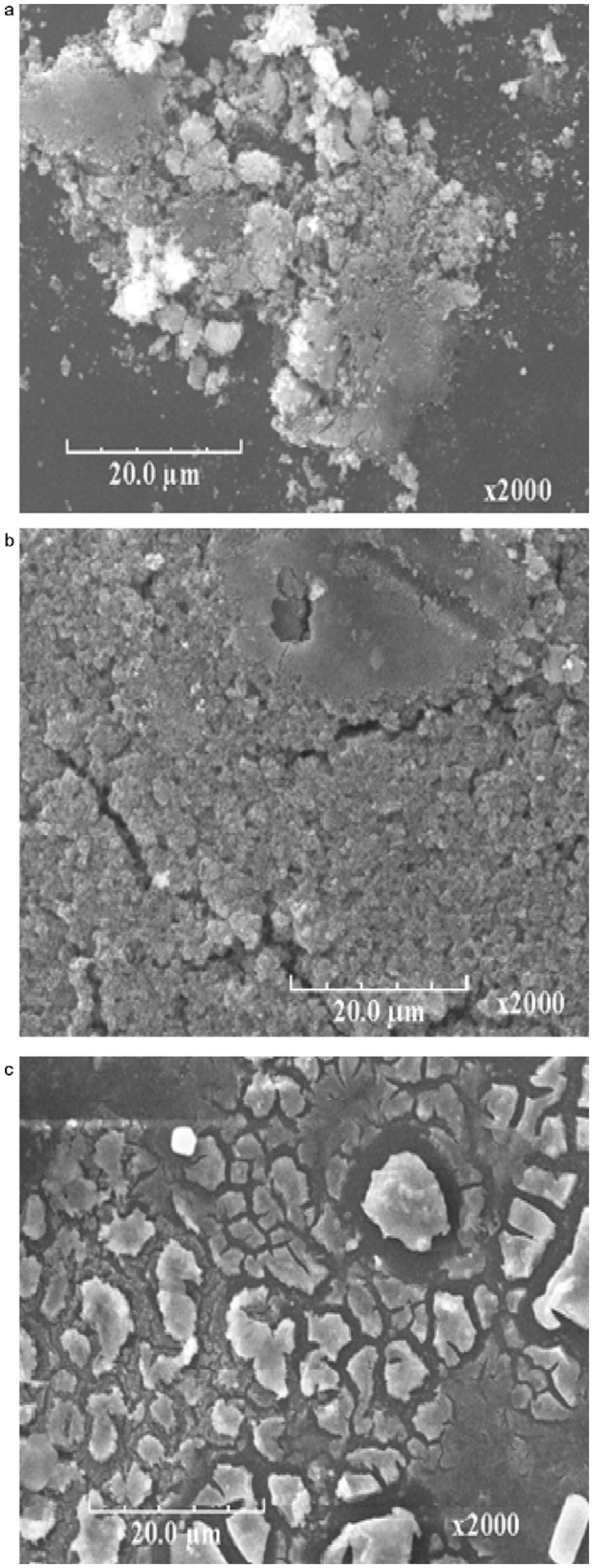

Fig. 6. (a) SEM diagrams for coupled WO_3/TiO_2 catalysts prepared by Procedure 3: unloaded TiO_2, (b) SEM diagrams for coupled WO_3/TiO_2 catalysts prepared by procedure 1: 0.5% – WO_3 loaded TiO_2 and (c) 2.5% – WO_3 loaded TiO_2, (c) SEM diagrams for coupled WO_3/TiO_2 catalysts prepared by Procedure 1: 4% – WO_3 loaded TiO_2.

Table 1
Percentage of anatase and rutile estimated from XRD software in the coupled TiO_2/WO_3 powders.

Percent of WO_3	Crystalline phases
0	91% anatase; 9% rutile
0.5	80% anatase; 20% rutile
0.75	79% anatase; 21% rutile
1	74% anatase; 26% rutile
1.25	74% anatase; 26% rutile
2	77% anatase; 23% rutile
2.5	79% anatase; 21% rutile

[8]. Similar observations were found for coupled WO_3/TiO_2 systems where the monoclinic phase expected to be formed at 400 °C [19] was not detected by XRD analysis with small amounts of WO_3 [7,8,19,20].

Since no new crystal phases were found and no shift was observed in the anatase and rutile peaks position, It can be supposed that no new solid was formed [7,20]. Also firing of the TiO_2/WO_3 samples at only 450 °C is known to be not sufficient to obtain solid solution between TiO_2 and WO_3 which is achieved above 1000 °C [13]. WO_3 is consequently not doping the TiO_2 lattice but is clustered on the surface of TiO_2. Similar results were reported in ref [7]. The impregnated WO_3 was spread on the surface of TiO_2 for the coupled catalysts heat treated at 400 °C for 2 h such as in Ref. [20], where the coupled TiO_2/WO_3 films prepared via sol–gel method and annealed at 500 °C, are shown to be a mixture of two phases [20]. Even for other TiO_2 doping element (the ITO semiconductor), ITO particles surrounded the TiO_2 without entering its lattice [23].

3.2. *Photocatalytic degradation under visible light*

3.2.1. *Films prepared by Procedure 1*

Photodegradation of SA under white light, using films prepared by Procedure 1 with WO_3 loadings up to 2.5 wt.%, followed a first order kinetics (Fig. 7a). The loadings up to 2 wt.% exhibited a negative effect on the photocatalytic activity. However, at 2.5 wt.% of WO_3 loading, a noticeable improvement of the kinetic was observed with an apparent first order kinetics constant of 25×10^{-4} min^{-1} against 18×10^{-4} min^{-1} for unloaded TiO_2 (Fig. 7b). SA removal after 300 min of irradiation had a similar trend: 51% of SA removal was observed using 2.5 wt.%-WO_3/TiO_2 against 42% for unloaded TiO_2 (Fig. 7c). At higher WO_3 loading and particularly for 3 wt.% of WO_3, there is no remarkable variation in the photocatalytic activity which slightly decreases in comparison with 2.5 wt.% (Fig. 7a). Authors have reported an adverse effect of high WO_3 loading mainly due to the decrease in the rate of oxygen reduction on the TiO_2 surface [8,12].

The first key reason for the enhancement of the photocatalytic activity at 2.5 wt.% of WO_3 is the red-shift of absorption wavelength range for coupled WO_3/TiO_2, which induces lower E_g of the system supposed to be easily excited by the visible light (Fig. 3c).

The absence of tungsten oxide peaks in the XRD spectra of the most active film 2.5 wt.%-WO_3/TiO_2 suggests that the increased photoactivity, with respect to TiO_2, is not due to the formation of crystalline tungsten oxide but is probably due to WO_3 acting as a separation centre for the electrons and holes.

Theoretically, the energy coming from the white light can both excite the semiconductor WO_3, which absorb wavelengths under 450 nm [8], and the rutile-TiO_2 (band edge 412 nm; 3 eV [21]). Electrons are then promoted to their conduction bands and holes are created in their valence bands, while anatase–TiO_2 particles are still not excited with electrons accumulated in their valence band only. Loading TiO_2 by WO_3 consists in the juxtaposition of particles of the two semiconductors which have different energy levels of the valence and conduction bands: this contributes to a charge transfer between the particles. According to the literature, the conduction and valence bands of WO_3 are lower in energy than those of TiO_2, the flat band potentials of TiO_2 and WO_3 are −0.1 and +0.5 V (vs. normal hydrogen electrode at pH 0) [15,20,26].

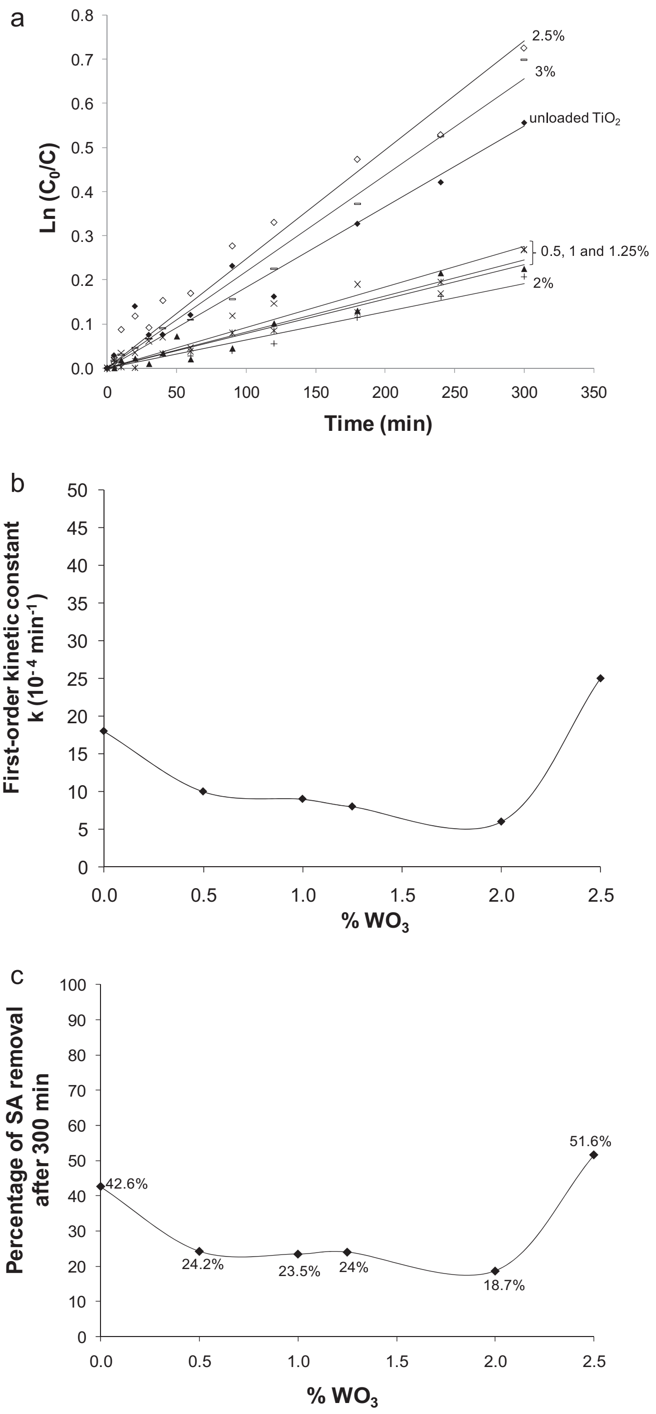

Fig. 7. (a) Photodegradation of SA under white light for catalysts prepared by Procedure 1 Linear transform $\ln(C_0/C)$ versus irradiation time (WO_3 loadings are indicated), (b) photodegradation of SA under white light for catalysts prepared by Procedure 1, apparent first order constants, and (c) photodegradation of SA under white light for catalysts prepared by Procedure 1, removal of SA after 300 min of irradiation.

Then, two phenomena may occur simultaneously depending on the contact of WO_3 with the allotropic phases of TiO_2.

The first one is a double way charge transfer between WO_3 and rutile-TiO_2, where photogenerated electrons are transferred from the conduction band of illuminated rutile-TiO_2 down to the lower-lying conduction band of WO_3 [8], whereas photogenerated holes remained on WO_3 or are transferred to the valence band of rutile-TiO_2 [8,20]. The second phenomenon is a one way charge transfer between WO_3 and anatase–TiO_2, where photogenerated holes in the valence band of WO_3 only can be transferred to the upper-lying valence band of non illuminated anatase–TiO_2.

This charge transfer results in a better electron/hole separation and is the second key reason for the observed higher efficiency of 2.5 wt.%-WO_3/TiO_2 system.

If we consider that unloaded TiO_2 is hardly activated by the white lamp since only 10% of the system corresponding to the amount of rutile phase can be photoexcited, logically the introduction of WO_3 which increased the amount of rutile could only enhance the photocatalytic activity, but experiments show inhibition at some loading amounts. The exact reason(s) for the observed inhibition remains unclear, especially when the supposed negative effect of WO_3 presented by some authors occurs only with excessively loaded TiO_2/WO_3 which was not the case in our experience [21]. considering at the observed decrease in photocatalytic activity, one should put the emphasis on the importance of the contact between the WO_3 and TiO_2 particles.

It should be noted that literature is replete with a better photocatalytic performance in coupled WO_3/TiO_2 systems using a visible light source [7–9,13,14,19,21].

The loading amount of 2.5 wt.% WO_3 used in this study is close to the optimal value found by many authors (3 wt.% [9,13,14]), but determining of such an optimal value was not a priority in this work since many different values of this optimum can be seen in the literature. We can only confirm from the bibliographic research that the enhancement of photocatalytic performance occurs only with adding low amounts of WO_3 (between 0.5 wt.% and 5 wt.%) [7,9,12–14,19,20].

3.2.2. Films prepared by Procedures 2 and 3

As it can be seen in Fig. 8, the films of coupled catalysts prepared by spin coating machine (Procedures 2 and 3) generally exhibits a higher photocatalytic performance with visible light than the one prepared by simple deposition of catalyst (Procedure 1) in spite of the less important deposed mass for films prepared with Procedures 2. This result can be explained by the enhanced light exposure of the semiconductor particles and/or the effective charge transfer related to a better dispersion of WO_3 in the TiO_2–WO_3 system, obtained by spin coating deposition.

Furthermore, behavior with WO_3 loading is different from that of Procedure 1: the same photocatalytic inhibition was observed for loadings from 0.5 wt.% to 2.5 wt.% for Procedure 2, but a continuous enhancement of photocatalytic performance was found for films prepared by sol–gel method (Procedure 3). The loading amount of WO_3 was extended consequently to 5 wt.% to find the optimum. 4 wt.% was the optimal loading, where the SA removal after 300 min of irradiation was more than 70%, which was 1.5 times higher than unloaded TiO_2 and represented the highest removal obtained under white lamp for the three procedures (Fig. 8b). This high activity may be directly linked to the lower band gap energy (2.3 eV) measured for catalyst at the same WO_3 loading.

The remarkable improvement of photocatalytic performance at 4 wt.% and 5 wt.% and the absence of the negative effect of WO_3 observed in the two first procedures, let us suppose that Procedure3, consisting in the introduction of tungsten precursor before sol–gel precipitation of TiO_2, is an interesting method to obtain the researched positive effect of WO_3: the introduction of the WO_3 precursor before the formation of TiO_2 crystals may be the best way to ensure good contact between the two semiconductors.

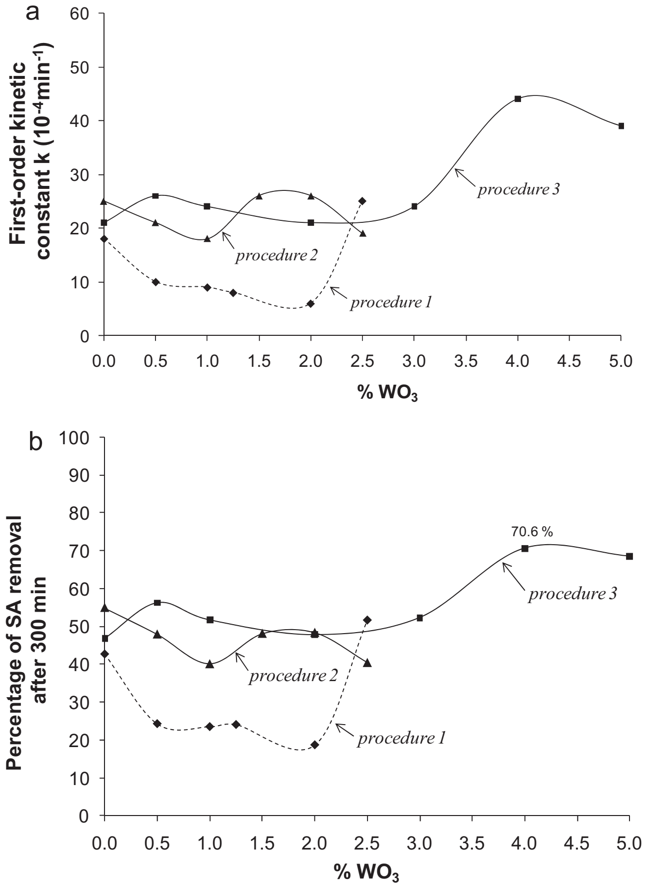

Fig. 8. (a) Photocatalytic performances of WO_3-loaded TiO_2 films prepared by different procedures for the SA photocatalysis under visible light, apparent first order constants; (b): Photocatalytic performances of WO_3-loaded TiO_2 films prepared by different procedures for the SA photocatalysis under visible light, % of SA removal after 300 min of irradiation.

3.3. Photocatalytic degradation under UV light

3.3.1. Films prepared by Procedure 1

The photo-oxidative transformation of SA followed first-order kinetics. The performances were generally higher under UV light than under white light (see Figs. 7 and 9). It is regular result since UV light is more powerful and excites TiO_2 which is the major compound present in the WO_3/TiO_2 system, and a lot of studies have also reported similar result [7,19].

The positive effect of WO_3 was observed especially at 0.5 wt.% WO_3 loading with more than 97% of SA removal after 300 min of irradiation (against 64.7% for unloaded TiO_2) and an apparent first order kinetics constant four times higher ($k = 120 \times 10^{-4}\ \text{min}^{-1}$) than the one for unloaded TiO_2 ($k = 33 \times 10^{-4}\ \text{min}^{-1}$) (Fig. 9). An enhancement of photocatalytic activity was also observed at 2.5 wt.% WO_3 loading, which confirms the result of the decrease in band gap energy at this loading to 2.6 eV (see Fig. 4a).

The advantage of using 365 nm is that light energy could excite both TiO_2 and WO_3, simultaneous electron transfer occurs then from TiO_2 to WO_3 and hole transfer in the opposite direction [7,8,15,20]. WO_3 acts consequently as an effective separation centre and enhancement of photocatalytic activity is expected. This trend was clearly observed in the SA photodegradation under UV light (Fig. 9) and 0.5 wt.% was the optimal value of WO_3 loading. Others have also noticed a positive effect of coupling WO_3 to TiO_2 under UV light [7,12,19–21], but the value of the optimal molar ratio of WO_3 differed between the authors, which can be expected

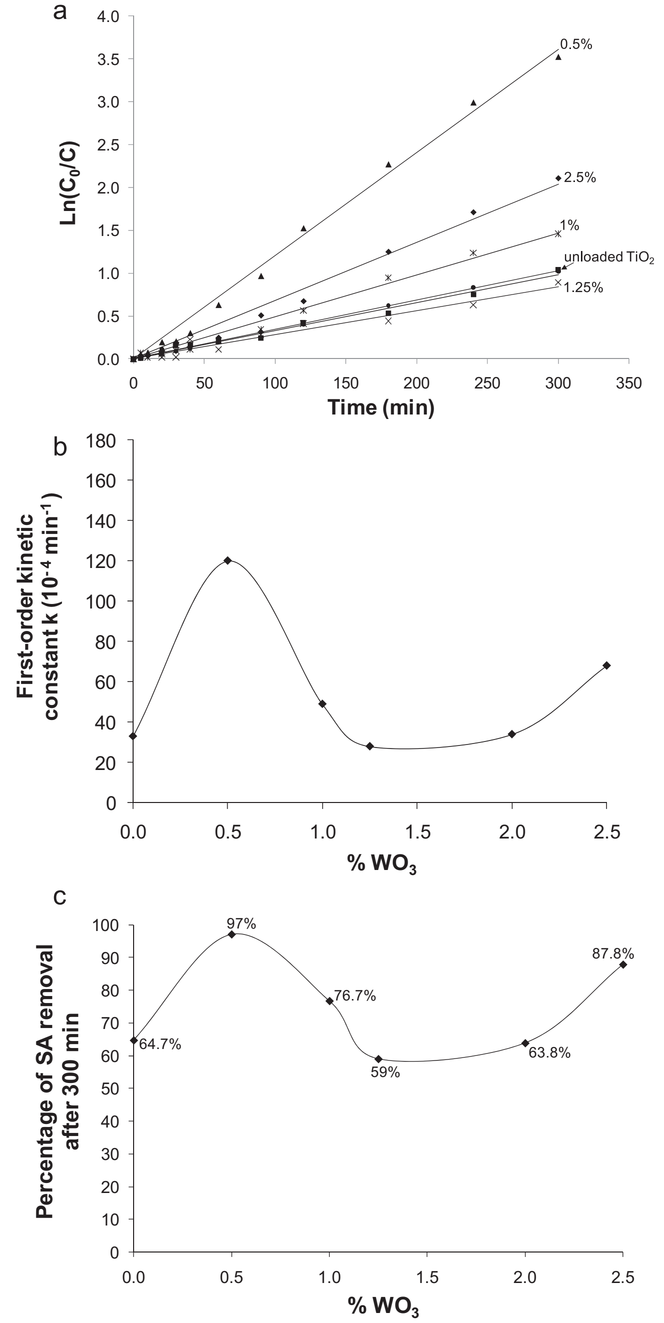

Fig. 9. (a) Photodegradation of SA under UV light for catalysts prepared by Procedure 1, Linear transform $\ln(C_0/C)$ versus irradiation time (WO_3 loadings are indicated), (b) photodegradation of SA under UV light for catalysts prepared by Procedure 1, apparent first order constants, and (c) photodegradation of SA under UV light for catalysts prepared by Procedure 1, removal of SA after 300 min of irradiation.

as the operating conditions during the coupling procedure were different.

3.3.2. Films prepared by Procedures 2 and 3

The main observation from the comparison between the behaviors of loaded films prepared by the three procedures is that films of Procedure1 exhibits the best photocatalytic performance under UV light. It can also be seen from Fig. 10 that 0.5 wt.%WO_3 loading is the common optimal ratio for the three procedures with the highest activity with a drastic decrease in the activity just beyond this loading value. Finally, it can be noticed that the increase in the photocatalytic activity observed for 4 and 5 wt.% loaded catalysts prepared by Procedure 3 is in accordance with the decrease in their band gap energy already observed in Fig. 4b.

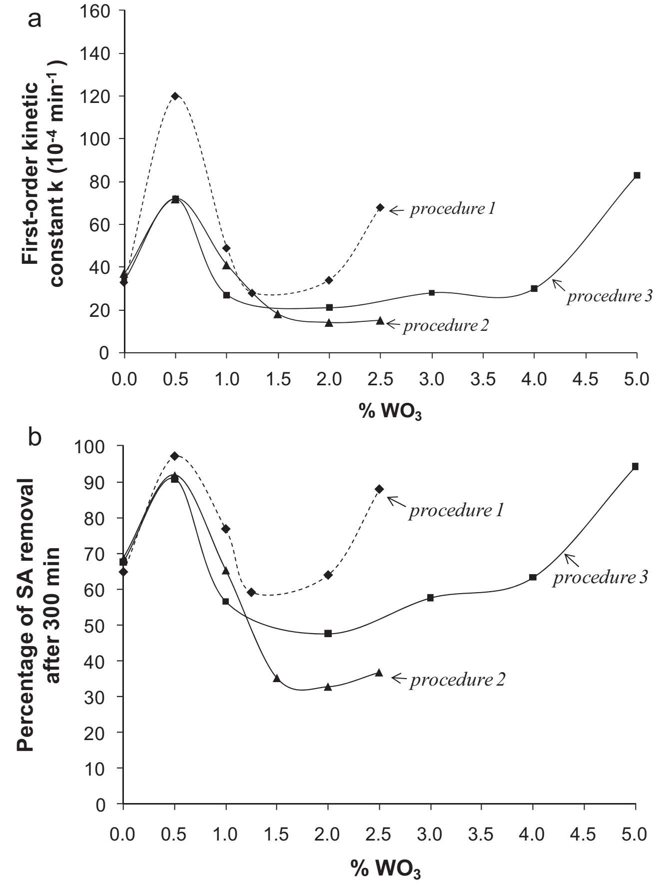

Fig. 10. (a) Photocatalytic performances of WO_3-loaded TiO_2 films prepared by different procedures for the SA photocatalysis under UV light, apparent first order constants, (b) photocatalytic performances of WO_3-loaded TiO_2 films prepared by different procedures for the SA photocatalysis under UV light, % of SA removal after 300 min of irradiation.

4. Conclusions

Novelty of this work consists in the production by different methods of new photocatalysts able to obtain a relevant removal rates of salicylic acid particularly in the visible light, coupled WO_3/TiO_2 photocatalysts were prepared by three different procedures: simple deposition on glass substrate of suspended catalysts loaded by incipient wetness method, spincoating deposition of TiO_2 P25 in viscous solution and finally spincoating deposition of TiO_2 prepared by sol–gel method, whereas WO_3 was introduced using different precursors. The important findings of this study are presented below.

- The absorbance edge shifted to the visible wavelengths after WO_3 loading for catalysts prepared by Procedure 1, the gap energy decreasing accordingly to 2.6 eV for 2.5 wt.% WO_3/TiO_2 loaded catalysts, while coupled catalysts prepared by Procedure 2 exhibited similar UV spectra to those of unloaded TiO_2 and no change was found in the band gap (3.1 eV). However, a drastic decrease of the band gap energy was measured for catalysts prepared by sol–gel method for 4 wt.% and 5 wt.% WO_3 loading, this

observation was in agreement with the observed photocatalytic enhancement at these loadings.
- A more transparent aspect was obtained for catalysts prepared by spincoating method, but adhesion on the glass substrate was not excellent compared to ones prepared by Procedure 1.
- A more uniform morphology and bigger agglomeration size was observed at 2.5 wt.% loading for catalysts prepared by Procedure 1, but the crystal phase of TiO_2 was not changed and new crystal phases were not found. XRD analysis demonstrated that WO_3 was not doped into the TiO_2 lattice but was clustered on the surface of TiO_2.
- Loading by WO_3 increased the amount of rutile in the WO_3/TiO_2 catalysts prepared by Procedure 1, which can be activated by the white lamp. In spite of that, an inhibition in photocatalytic activity was noted for some loading amounts. The photocatalytic performance cannot be linked to the amount of rutile.
- Under white lamp irradiation, an initial inhibition followed by an enhancement of the photocatalytic performances at 2.5 wt.% of WO_3 was observed for coupled catalysts prepared by Procedure 1; a one way ($WO_3 \Rightarrow$ anatase–TiO_2) and/or two ways (rutile-$TiO_2 \Leftrightarrow WO_3$) charge transfer occurs resulting in a better electron/hole separation. Contrarily a continuous enhancement of photocatalytic performance was observed for films prepared by sol–gel method (Procedure 3) after WO_3 addition until 4 wt.%, which represented the optimal loading. Films of coupled catalysts deposited by spincoating machine (Procedures 2 and 3) exhibited generally higher photocatalytic performance than ones prepared by simple deposition method with visible light, it can be supposed that this method enhances the accessibility of photons to the catalyst particles.
- Photocatalytic performances were generally higher under UV light than under white lamp for all the coupled catalysts prepared by the different procedures. The positive effect of loading by WO_3 was also noted under UV irradiation, where a two ways charge transfer occurs between the two activated semiconductors. 0.5 wt.% WO_3 was the common optimal ratio for the catalysts prepared by the three different procedures.

Acknowledgment

The authors gratefully acknowledge the financial support of the “Agence Universitaire de la francophonie”.

References

[1] E. Evgenidou, K. Fytianos, I. Poulios, J. Photochem. Photobiol. A 175 (2005) 29–38.
[2] C.H. Ao, S.C. Lee, J.Z. Yu, J.H. Xu, Appl. Catal. B 54 (2004) 41–50.
[3] M.R. Ghezzar, F. Abdelmalek, M. Belhadj, N. Benderdouche, A. Addou, Appl. Catal. B 72 (2007) 304–313.
[4] M. Ismail, L. Bousselmi, Water Sci. Technol. 61 (10) (2010) 2539–2548.
[5] L. Bousselmi, S.U. Geissen, H. Schroeder, Water Sci. Technol. 49 (4) (2004) 331–337.
[6] I. Justicia, P. Ordejon, G. Canto, J.L. Mozos, J. Fraxedas, G.A. Battiston, Adv. Mater. 14 (2002) 1399–1402.
[7] C. Shifu, C. Lei, G. Shen, C. gengyu, Powder Technol. 160 (2005) 198–202.
[8] C.F. Lin, C.H. Wu, Z.N. Onn, J. Hazard. Mater. 154 (1–3) (2008) 1033–1039.
[9] X.Z. Li, F.B. Li, C.L. Yang, W.K. Ge, J. Photochem. Photobiol. A 141 (2001) 209–217.
[10] M. Saadoun, H. Chorfi, L. Bousselmi, B. Bessaïs, Phys. Status Solidi C4 (2007) 2029.
[11] V. Iliev, D. Tomova, L. Bilyarska, L. Prahov, L. Petrov, J. Photochem. Photobiol. A 159 (2003) 281–287.
[12] V. Keller, P. Bernhardt, F. Garin, J. Catal. 215 (2003) 129–138.
[13] Y.T. Kwon, K.Y. Song, W.I. Lee, G.J. Choi, Y.R. Do, J. Catal. 191 (2000) 192–199.
[14] Y.R. Do, W. Lee, K. Dwight, A. Wold, J. Solid State Chem. 108 (1994) 198–201.
[15] N. Serpone, P. Maruthamuthu, P. Pichat, E. Pellizetti, H. Hidaka, J. Photochem. Photobiol. A 85 (1995) 247–255.
[16] R.A. Doong, C.H. Chen, R.A. Maithreepala, S.M. Chang, Water Res. 35 (12) (2001) 2873–2880.
[17] Q.J. Lui, X.K. Yang, J. Inorg. Mater. (2003) 1331–1336.
[18] R. Suárez-Parra, I. Hernández-Pérez, M.E. Rincón, S. López-Ayala, M.C. Roldán-Ahumada, Sol. Energy Mater. Sol. Cells 76 (2) (2003) 189–199.
[19] B. Tryba, M. Piszcz, A.W. Morawski, Int. J. Photoenergy (2009) (Article ID 297319).
[20] A. Rampaul, I.P. Parkin, S.A. O'Neill, J. DeSouza, A. Mills, N. Elliott, Polyhedron 22 (2003) 35–44.
[21] F. Bosc, D. Edwards, N. keller, V. Keller, A. Ayral, Thin Solid Films 495 (2006) 272–279.
[22] S.M. Ould-Mame, O. Zahraa, M. Bouchy, Int. J. Photoenergy 2 (2000) 59–66.
[23] H. Chorfi, G. Zayani, M. Saadoun, L. Bousselmi, B. Bessaïs, Appl. Surf. Sci. 256 (2010) 2170–2175.
[24] J. Engweiler, J. Harf, A. Baiker, J. Catal. 159 (1996) 259–269.
[25] M.J. Scotter, D.P.T. Roberts, L.A. Wilson, F.A.C. Howard, J. Davis, N. Mansell, Food Chem. 105 (2007) 273–279.
[26] D. Robert, Catal. Today 122 (2007) 20–26.
[27] O. Zahraa, S. Maire, F. Evenou, C. Hachem, M.N. Pons, A. Alinsafi, M. Bouchy, Int. J. Photoenergy (2006) 1–9 (Article ID 46961).
[28] H. Tada, A. Kokubu, M. Iwasaki, S. Ito, Langmuir 20 (2004) 4665–4670.
[29] S. Higashimoto, Y. Ushiroda, M. Azuma, Top. Catal. 47 (2008) 148–154.
[30] H.X. Li, R.H. Xia, Z.W. Jiang, S.S. Chen, D.Z. Chen, Chin. J. Chem. 26 (2008) 1787–1792.
[31] H. Gnaser, B. Huber, C. Ziegler, Encyclopedia Nanosci. Nanotechnol. American Scientific Publishers; ISBN: 1-58883-062-4, 6 (2004) 505–535.
[32] L. Li, J. Liu, Y. Su, G. Li, X. Chen, X. Qiu, T. Yan, Nanotechnology 20 (2009) 155706–155714.
[33] J.A. Navio, J.J. Testa, P. Djedjeian, J.R. Padron, D. Rodriguez, M.I. Litter, Appl. Catal. A: Gen. 178 (1999) 191–203.